Monocyte-Derived Macrophages Are Necessary for Beta-Adrenergic Receptor-Driven Choroidal Neovascularization Inhibition

Steven Droho,[1] Carla M. Cuda,[2] Harris Perlman,[2] and Jeremy A. Lavine[1]

[1]Department of Ophthalmology, Feinberg School of Medicine, Northwestern University, Chicago, Ilinois, United States
[2]Department of Medicine, Division of Rheumatology, Feinberg School of Medicine, Northwestern University, Chicago, Ilinois, United States

PURPOSE. Beta-adrenergic receptor (AR) antagonists, like propranolol, inhibit angiogenesis in multiple ocular conditions through an unknown mechanism. We previously showed that propranolol reduces choroidal neovascularization (CNV) by decreasing interleukin-6 levels. Since macrophages are one of the central producers of interleukin-6, we examined whether macrophages are required for propranolol-driven inhibition of choroidal angiogenesis.

METHODS. We tested the anti-angiogenic properties of propranolol in the choroidal sprouting assay and the laser-induced CNV model. Bone marrow-derived monocytes (BMDMs) were added to the choroidal sprouting assay and $Ccr2^{-/-}$ mice were subjected to laser-induced CNV. Multi-parameter flow cytometry was performed to characterize the ocular mononuclear phagocyte populations after laser injury and during propranolol treatment.

RESULTS. Propranolol reduced choroidal angiogenesis by 41% ($P < 0.001$) in the choroidal sprouting assay. Similarly, propranolol decreased laser-induced CNV by 50% ($P < 0.05$) in female mice, with no change in males. BMDMs increased choroidal sprouting by 146% ($P < 0.0001$), and this effect was ablated by propranolol. Beta-AR inhibition had no effect upon laser-induced CNV area in female $Ccr2^{-/-}$ mice. MHCII$^+$ and MHCII$^-$ macrophages increased 20-fold following laser treatment in wildtype mice as compared to untreated mice, and this effect was completely attenuated in lasered $Ccr2^{-/-}$ mice. Moreover, propranolol increased the numbers of MHCII$^+$ and MHCII$^-$ macrophages by 1.9 ($P = 0.07$) and 3.1 ($P < 0.05$) fold in lasered female mice with no change in macrophage numbers in males.

CONCLUSIONS. Our data suggest that propranolol inhibits angiogenesis through recruitment of monocyte-derived macrophages in female mice only. These data show the anti-angiogenic nature of beta-AR blocker-recruited monocyte-derived macrophages in CNV.

Keywords: macrophage, adrenergic receptor, choroidal neovascularization

Over the last 10 years, the use of beta-adrenergic receptor (beta-AR) blockers has expanded to include multiple anti-angiogenic indications within ophthalmology. Leaute-Labeze et al. first reported the tumor regressive properties of the non-specific beta-AR blocker propranolol in severe hemangioma of infancy.[1] Additionally, systemic[2] and topical[3] propranolol regresses pre-threshold retinopathy of prematurity. Furthermore, patients on aqueous suppressants (including beta-AR blockers such as timolol) demonstrate improved visual acuity and reduced retinal thickness compared to controls in the comparison of age-related macular degeneration (AMD) treatments trial.[4] Finally, adjuvant topical dorzolamide-timolol improves retinal thickness in patients with neovascular AMD on maximal anti-vascular endothelial growth factor (VEGF) therapy.[5,6]

Despite the clinical efficacy of beta-AR antagonists in angiogenic eye diseases such as neovascular AMD, its mechanism of action is poorly understood. Isolated hemangioma cells demonstrate reduced VEGF protein levels after culture with propranolol,[7] but immunohistochemical analysis revealed no change in VEGF or VEGF receptor expression of surgically excised hemangiomas,[8] suggesting alternative mechanisms. We previously showed that propranolol inhibits laser-induced choroidal neovascularization (CNV) by 50%.[9] Additionally, reduced CNV area correlates with a decrease in the ocular level of the proinflammatory cytokine, interleukin-6, while the levels of VEGF remain unchanged.[10] Since macrophages are known to be large producers of interleukin-6, we examined whether propranolol-driven CNV inhibition is mediated by macrophages. Macrophage depletion has already been shown to significantly reduce laser-induced CNV area,[11,12] and the beta2-AR is necessary for particulate matter-triggered interleukin-6 expression in lung macrophages.[13]

In this report, we investigated the mechanism of propranolol-mediated suppression of choroidal angiogenesis. Propranolol reduced the laser-induced CNV area in female but not male mice. Additionally, propranolol failed to inhibit laser-induced CNV in female C-C chemokine receptor type 2 (CCR2) knockout mice. Finally, propranolol increased macrophage recruitment to laser lesions in female but not male mice. These data suggest that beta-AR antagonist-driven recruitment of monocyte-derived macrophages are necessary for inhibition of
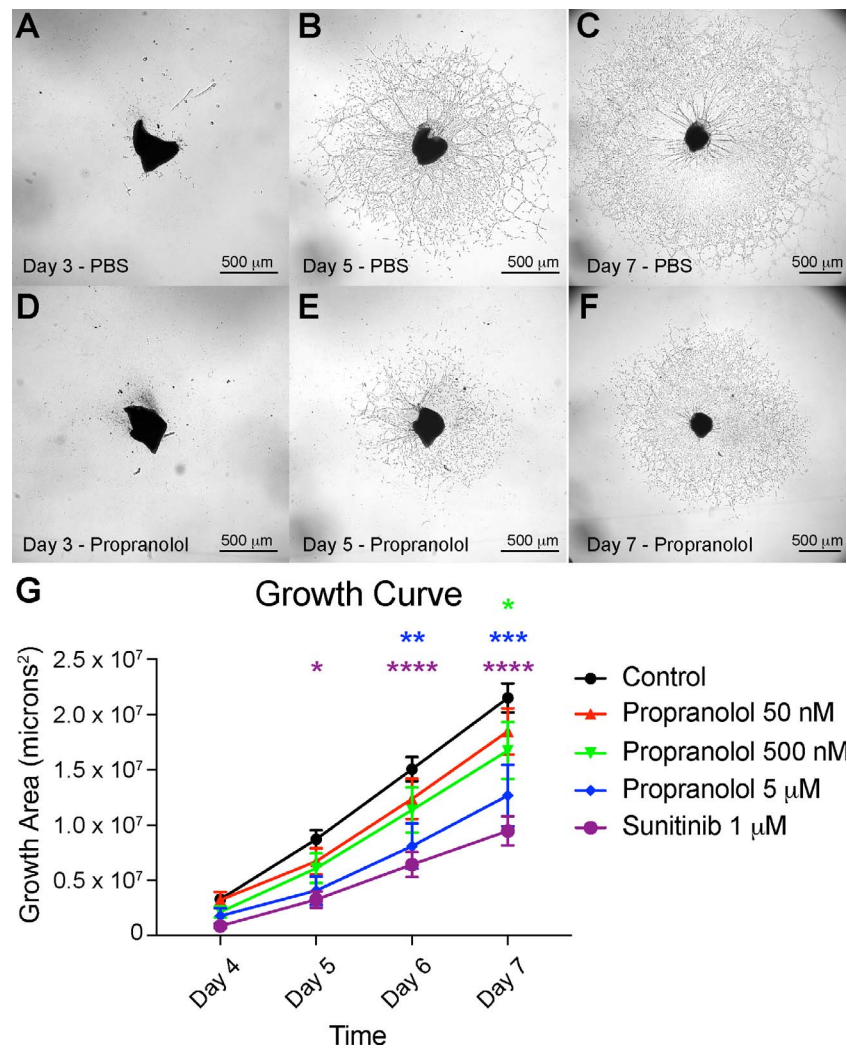
FIGURE 1. Propranolol inhibits choroidal angiogenesis in the ex vivo sprouting assay. Representative photos of vehicle (PBS, [A–C]) and propranolol 5 µM (D–F) treated choroidal explants on Day 3, Day 5, and Day 7. (G) Choroidal angiogenesis growth curve from Day 4–Day 7 ($N = 6–12$ per group, $^{*}P < 0.05$, $^{**}P < 0.01$, $^{***}P < 0.001$, $^{****}P < 0.0001$ compared to control, *color of symbol* identifies comparison to control).

CNV and that macrophage recruitment explains the sex-specific effects of beta-AR inhibitors.

METHODS

Mice

All experiments were conducted in accordance with the ARVO Statement for the Use of Animals in Ophthalmic and Vision Research and were approved by the Northwestern University Institutional Animal Care and Use Committee. C57BL/6J wildtype (#664) and $Ccr2^{-/-}$ (#4999) mice were purchased from The Jackson Laboratory (Bar Harbor, ME, USA). Mice were bred in-house and maintained in a pathogen-free barrier facility within Northwestern University's Center for Comparative Medicine. Any animals received directly from The Jackson Laboratory were housed for at least 2 weeks before use. All experiments were performed at 10 to 12 weeks of age. Genotypes of all mice, including the absence of the *Rd8* mutation, were confirmed by services provided by Transnetyx, Inc. (Cordova, TN, USA).

Choroidal Sprouting Assay

Eyes were carefully enucleated and placed in ice-cold PBS. Eyes were dissected in EGM2-MV supplemented (hydrocortisone was omitted) medium (CC3202; Lonza, Walkersville, MD, USA) into posterior eye cups containing sclera, RPE, and choroid complex. The peripheral choroid was separated from the central choroid, cut into 0.5 mm × 0.5 mm pieces, and placed into growth factor reduced Matrigel (#356231; Corning, Bedford, MA, USA) in a 48-well plate on ice. The Matrigel was solidified by incubating at 37°C for 10 minutes. EGM2-MV medium was changed every 2 days. Sunitinib (PZ0012) and propranolol (P0884) were purchased from Sigma (St. Louis, MO, USA). Sunitinib was added on Day 0, and propranolol was added on either Day 0 or Day 2. Pictures were taken on a Nikon Ti2 Widefield microscope (Buffalo Grove, IL, USA) using a 4× objective and Nikon NIS Elements software. Images were analyzed with the Nikon Elements General Analysis. Images were preprocessed with edge detection and segmented with thresholding. The largest area was measured for each image. The central choroidal tissue area was subtracted from the total angiogenesis area.
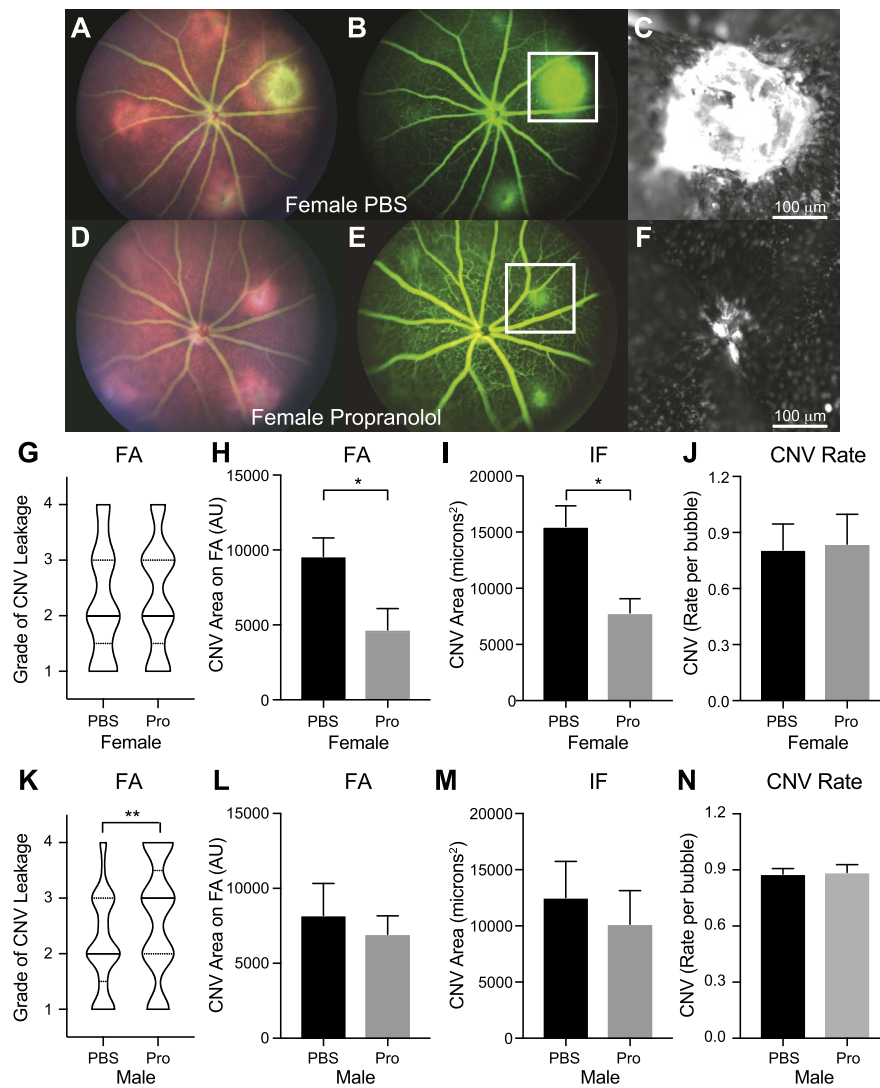
FIGURE 2. Propranolol reduces laser-induced CNV area in female mice. Representative fundus photography, FA, and IF images from PBS- (**A–C**) and propranolol-treated (**D–F**) female mice on Day 14. CNV leakage grading on FA (**G**) was not changed in female mice (*violin plot with solid line indicating median*; *dashed lines indicated quartiles*; $N = 48$–49 lesions per group). CNV area on FA (**H**) and IF (**I**) was reduced by 50% in female mice with no change in CNV rate (**J**, $N = 6$–7 mice per group, *$P < 0.05$). CNV leakage grading on FA was increased by propranolol in male mice (**K**, **$P < 0.01$, $N = 80$–86 lesions per group). CNV area (**L**, **M**) and CNV rate (**N**) were unchanged in male mice ($N = 10$–11 mice per group).

Bone Marrow-Derived Monocyte (BMDM) Isolation

Mice were killed and hind limbs were removed while maintaining integrity of the hip joint. Legs were kept in DMEM (#10-013-CV; Corning, Manassas, VA, USA) on ice until removal of muscles. The femur and tibia were cut proximal to the joint before flushing bone marrow with DMEM applied via a syringe fitted with a 21G needle. Flushed bone marrow was pushed through a 40 μm filter (#352340; Falcon, Durham, NC, USA) with a syringe plunger, and the filter was rinsed with additional DMEM. Cells were spun at 350g for 15 minutes and then passed through a second 40 μm filter. Monocytes were isolated from whole bone marrow using a negative selection magnetic bead protocol from Miltenyi Biotec (#130-100-629; Auburn, CA, USA) where non-monocytes were antibody labeled and positively selected via a magnetic column, while the non-labeled monocyte-enriched fraction was isolated from the flow through (LS 130-042-401; Miltenyi Biotec). Isolated BMDMs were counted and added to the choroidal sprouting assay in EGM2-MV medium on Day 2.

Laser-Induced CNV

Mice were anesthetized via intraperitoneal (IP) delivery of ketamine (90 mg/kg; Akorn, Lake Forest, IL, USA)/xylazine (12 mg/kg; Akorn) cocktail. Eyes were anesthetized with 1 drop of 0.5% tetracaine (Alcon, Fort Worth, TX, USA). Pupils were dilated with 1 drop of 2.5% phenylephrine (Akorn) and 0.5% tropicamide (Akorn). The whiskers were trimmed with scissors. A subcutaneous injection of meloxicam (1 mg/kg; Henry Schein Animal Health, Melville, NY, USA) was given for pain control. Mice were moved to the slit lamp stage and a cover slip was coupled to the cornea using Goniosoft (OCuSOFT, Rosenberg, TX, USA) to allow direct retinal visualization. Mouse eyes were treated with 4 (CNV area quantitation) or 8 (flow cytometry) focal laser burns (75 um, 110 mW, 100 msec) in each eye using an IRIDEX (Mountain View, CA, USA) 532 nm argon ophthalmic laser delivered via a Zeiss (Oberkochen, Germany) slit lamp. IP injections of propranolol (20 mg/kg) or PBS were performed daily during the course of experiments.
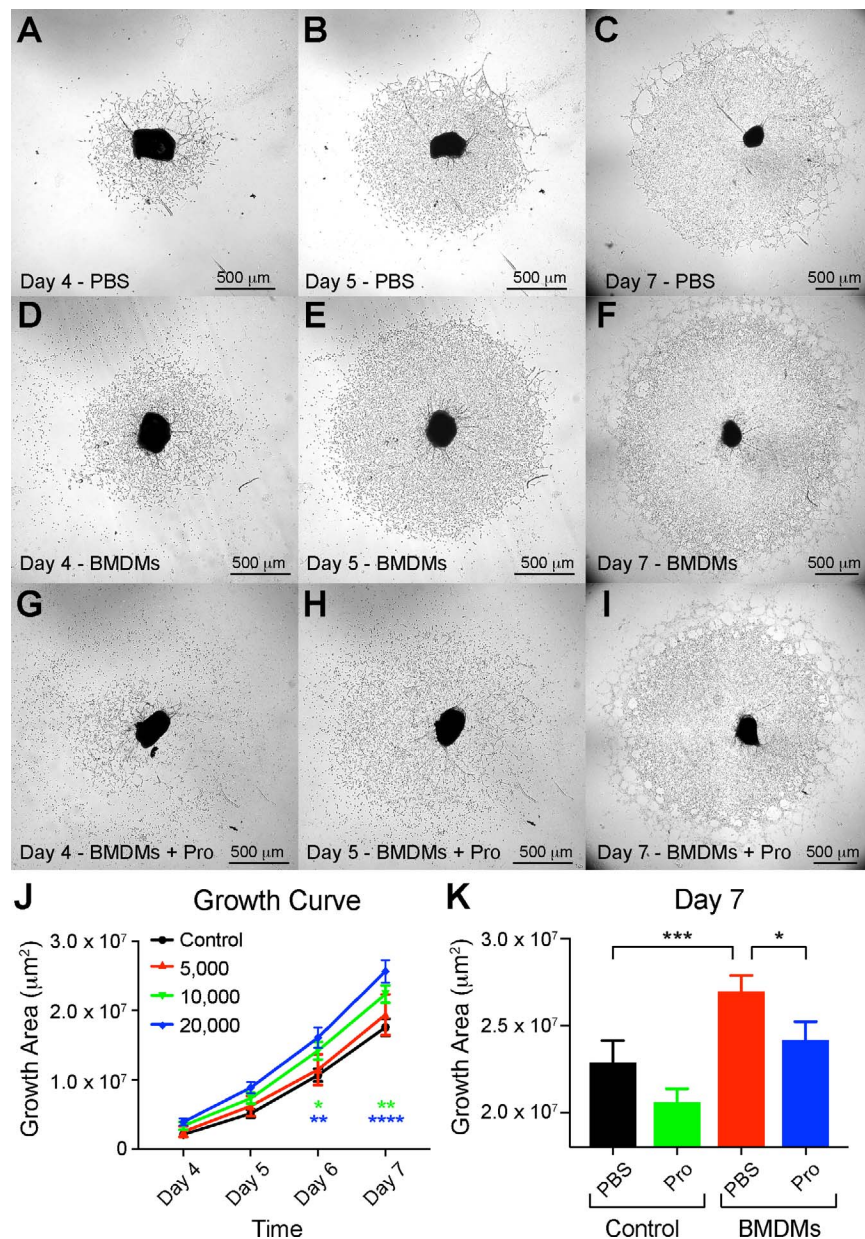
FIGURE 3. Propranolol blunts BMDM-stimulated choroidal angiogenesis in the ex vivo sprouting assay. Representative photos of PBS- (A–C), BMDM-treated (D–F), BMDM and propranolol-treated (1 μM, [G–I]) choroidal explants on Day 4, Day 5, and Day 7. The small cells around the explant are BMDMs (D, G), and are easily distinguishable from the microvascular angiogenesis of the explant. (J) Choroidal angiogenesis growth curve from Day 4–Day 7 ($N = 6$-12 per group, *$P < 0.05$, **$P < 0.01$, ****$P < 0.0001$ compared to control, *color of symbol* identifies comparison to control). (K) BMDM increase angiogenesis area on Day 7 (***$P < 0.001$), and this effect is inhibited by propranolol (*$P < 0.05$, $N = 11$-12 per group).

Fluorescein Angiography (FA) Imaging

Mice were anesthetized and prepped as described above on Day 14 after laser-induced CNV. Fluorescein (0.03–0.05 ml, 100 mg/ml; Akorn) was injected into the tail vein. The fundus was imaged using the Micron3 fundus camera (Phoenix Technology Group, Pleasanton, CA, USA). After imaging, mice were given ophthalmic ointment (Akorn) and placed in a heated recovery cage. Area of leakage was assessed by a reviewer blinded to treatment and genotype by using the freehand tool to draw a perimeter around the area of leakage and using the ROI manager to calculate an area in pixels via Fiji (NIH, Bethesda, MD, USA). Grading of leakage was assessed by two blinded reviewers using the 1–4 grading scale, as previously described.[14] Because we did not have early frames for every

eye, only late phase angiograms were scored and grade 2 was not assessed as 2A and 2B.[15] When the two blinded reviewers occasionally differed by 1 point, the scores were averaged.

Immunofluorescence (IF) Imaging

Mice were killed directly after FA imaging, and enucleated eyes were placed into 1% paraformaldehyde (#15713-S; Electron Microscopy Sciences, Hatfield, PA, USA) for 1 hour at room temperature. Eyes were moved to PBS; conjunctiva and optic nerve remnants were removed. A limbal incision was carried 360° to remove the cornea and iris. The lens and retina were carefully teased apart and discarded leaving a posterior eye cup of RPE, choroid, and sclera. Cups were blocked overnight in Donkey Serum Blocking Buffer (DSBB): Tris buffered saline
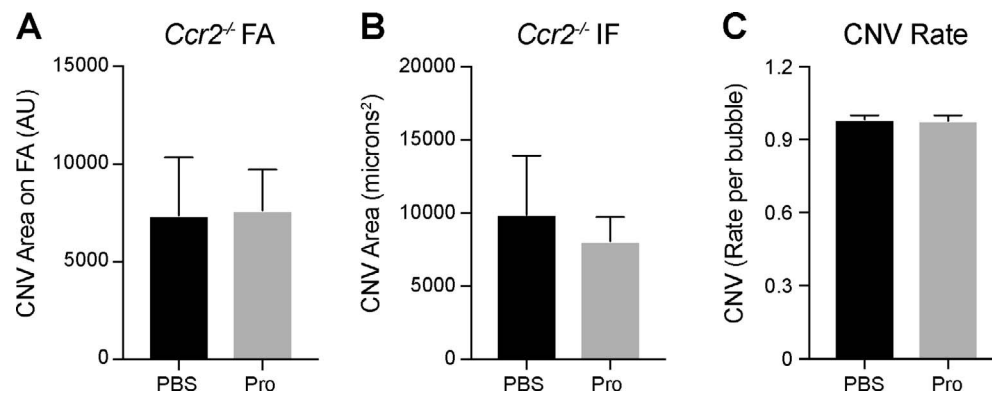
FIGURE 4. Propranolol has no effect upon laser-induced CNV area in the context of CCR2 inhibition or *Ccr2* deficiency. CNV area (**A**, **B**) and CNV rate (**C**) were unaffected by daily PBS or propranolol (20 mg/kg) in $Ccr2^{-/-}$ female mice (N = 7 per group).

(#BP2471, Fisher, Fair Lawn, NJ, USA) containing 5% donkey serum (S30, Sigma), 2.5% bovine serum albumin (A2153, Sigma), and 0.5% Triton X-100 (X100; Sigma). Eye cups were then incubated with anti-ICAM-2 antibody (Table) in DSBB overnight at 4°C before washing 5 times with TBS-T (TBS with 0.5% Tween-20, #00777; Amresco, Solon, OH, USA). Secondary antibody staining was performed with an Alexa Fluor 488-conjugated anti-rat antibody (Table) overnight at 4°C before washing 5 times with TBS-T containing 0.5% Tween-20 (Amresco). Eye cups were flat mounted on HistoBond microscope slides (16004-406, VWR; Batavia, IL, USA) in Immu-Mount (#9990402; ThermoFisher, Carlsbad, CA, USA). Pictures were taken on a Nikon Ti2 widefield microscope using Nikon NIS Elements software. Area of neovascularization was assessed by a blinded reviewer using the freehand tool to draw a perimeter around the area of leakage and an ROI manager to calculate an area in pixels via Fiji. Next, pixel area was transformed to microns^2 by multiplying by a factor related to pixel to micron ratio (in our case, 0.5249). CNV rate was calculated by determining the ratio of CNV lesions detected on FA and IF per mouse over the number of bubbles formed during the laser process.

Flow Cytometry

Enucleated eyes were minced into small pieces and digested using a mixture of Liberase TL (0.1 mg/ml, #5401020001; Roche, Basel, Switzerland) and DNase I (0.2 mg/ml, #10104159001; Roche) in HBSS (14025-092; Fisher) at 37°C for 60 minutes with mechanical digestion at time 0, 30, and 60 minutes via a gentleMACS Octo Dissociator (130-095-937; Miltenyi Biotec) in C-tubes (130-096-334; Miltenyi). Cells were filtered through 40 μm nylon mesh in MACS Buffer (130-091-221; Miltenyi). Cells were spun at 350g for 10 minutes and washed once in MACS Buffer. Erythrocytes were lysed using PharmLyse (1 minute, #555899; BD Biosciences) and washed once as above. Cells were stained for dead cells using Aqua Live/Dead (15 minutes, Table) and washed twice. Cells were incubated with Fc-Block (20 minutes, Table), stained with fluorochrome-conjugated Abs (30 minutes, Table), washed twice, fixed with 2% PFA and washed twice. Data were acquired on an LSR II flow cytometer (BD Biosciences). Compensation matrices and data analysis were performed using FlowJo (Tree Star, Ashland, OR, USA). Approximately 3,000,000 singlet events were counted per mouse (2 eyes). First, singlet cells were identified and dead cells were excluded. CD45, a marker of leukocyte lineage, was used to

TABLE. List of Antibodies Used for Flow Cytometry and Immunofluorescence

|	Fluorochrome	Clone	Company	Catalog #
Flow cytometry				
Fc block	–	–	BD Biosciences	553142
Aqua live/dead	AmCyan	–	ThermoFisher	65-0866-14
CD45	PE-Cy7	30-F11	BD Biosciences	552848
CD64	PE	X54-5/7.1	BD Biosciences	139304
CD11b	APC-Cy7	M1/70	BD Biosciences	557657
Ly6G	PECF594	1A8	BD Biosciences	562700
B220	PECF594	RA3-6B2	BD Biosciences	562313
NK-1.1	PECF594	PK136	BD Biosciences	562864
Siglec F	PECF594	E50-2440	BD Biosciences	562757
CD4	PECF594	RM4-5	BD Biosciences	562314
CD8	PECF594	53-6.7	BD Biosciences	562315
MHC II	Alexa fluor 700	M5/114.15.2	BioLegend	107622
CD31	APC	MEC 13.3	BD Biosciences	562861
CD140b	PerCP-Cy 5.5	APB5	ThermoFisher	17-1402-82
Immunofluorescence				
ICAM-2	–	3C4(mIC2/4)	BD Biosciences	553326
Donkey anti-Rat	Alexa fluor 488	Polyclonal	ThermoFisher	A21208
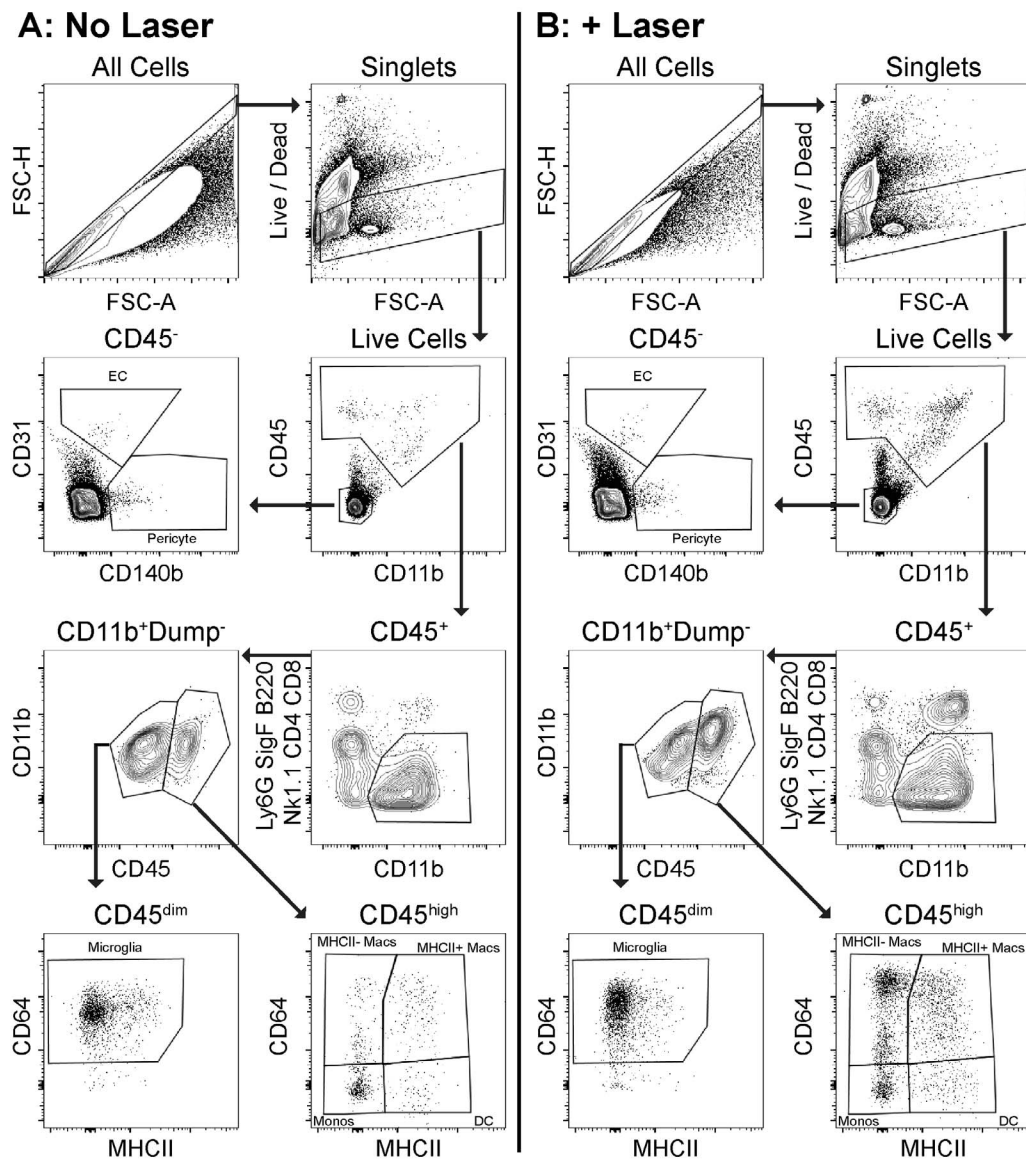
FIGURE 5. Flow cytometry gating strategy. Flow cytometry gating strategy for unlasered (**A**) and lasered (**B**) mice. Singlets were identified and gated forward. Dead cells were excluded. Live cells were separated into CD45$^-$ and CD45$^+$ populations. Endothelial cells (EC) were delineated by CD31+ staining and pericytes were identified by CD140b+ staining in CD45$-$ cells. Eosinophils, neutrophils, NK cells, T cells, and B cells were excluded by negative staining for SiglecF, Ly6G, NK1.1, CD4, CD8, and B220 (Dump gate). CD11b$^+$Dump$^-$ cells were separated into CD45^{dim} and CD45^{high} groups. Microglia were identified as CD64$^+$MHCII^{low} in the CD45^{dim} group. Macrophages were detected as CD64$^+$MHCII$^-$ (MHCII$^-$ Macs) and CD64$^+$MHCII$^+$ (MHCII+ Macs) in the CD45^{high} group. Monocytes were delineated as CD64$^-$MHCII$^-$, and dendritic cells (DC) were identified as CD64$^-$MHCII$^+$.

identify leukocytes versus non-leukocytes. CD45$^-$ non-leukocytes were gated on CD31 and CD140b to identify endothelial cells (EC) and pericytes, respectively. CD45$^+$ leukocytes were gated on CD11b$^+$ staining to identify mononuclear phagocytes and SiglecF, Ly6G, Nk1.1, B220, CD4, and CD8 negative staining to exclude eosinophils, neutrophils, NK cells, B cells, and T cells. Microglia have previously been shown to be CD45^{dim} and MHCII^{low} compared to infiltrating monocytes and macrophages.[16] Therefore, we used CD45^{dim} versus CD45^{high} to identify microglia from infiltrating cells. Microglia were identified in the CD45^{dim} group as CD64$^+$ and predominantly MHCII^{low}. In the CD45^{high} group, we identified CD64$^-$MHCII$^-$ monocytes, CD64$^-$MHCII$^+$ dendritic cells (DC), and two populations of macrophages: CD64$^+$MHCII$^-$ macrophages (MHCII$^-$ Macs) and CD64$^+$MHCII$^+$ macrophages (MHCII$^+$

Macs). Fluorescence minus one controls were used to establish positive staining and gates (Supplementary Fig. S1).

Statistical Analysis

Statistical analysis was performed using GraphPad Prism 8 (San Diego, CA, USA). Choroidal explants were analyzed using 2-way ANOVA (time and treatment) followed by Dunnett's or Tukey's multiple comparisons test. We used Dunnett's test when we were comparing only to control, and Tukey's test when comparing among all groups. Laser-induced CNV lesion areas were averaged for each mouse and compared using the Mann-Whitney U test because the data were non-parametrically distributed. FA leakage grading was analyzed by Mann-Whitney on a per lesion basis. Flow cytometry data were analyzed as percent live cells for each cellular population per mouse.
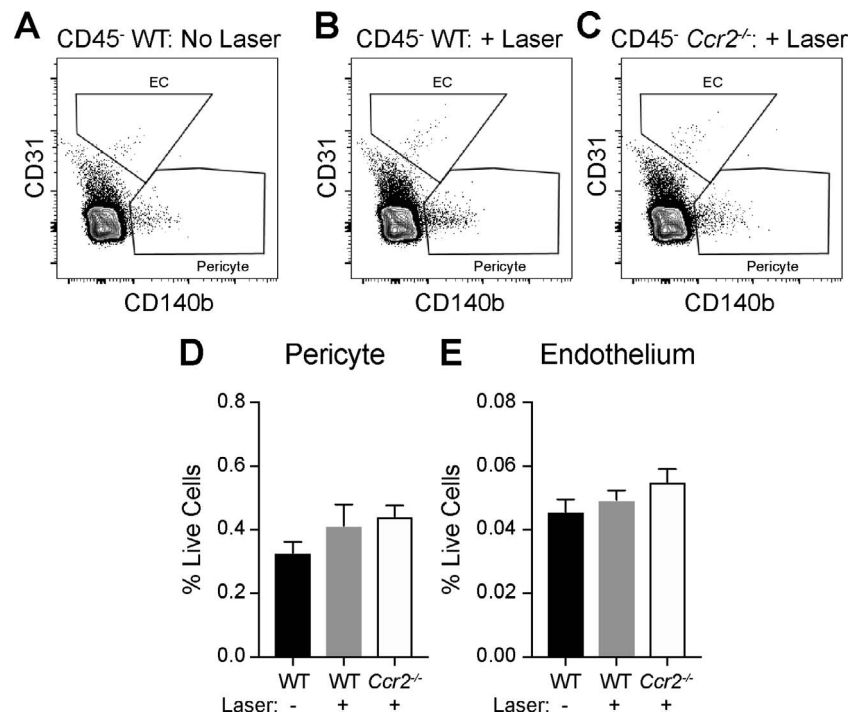
FIGURE 6. Pericytes and endothelial cells are unaffected by laser or *Ccr2*-deficiency. Representative flow cytometry plots of CD45⁻ cells in WT unlasered (**A**), WT lasered (**B**), and *Ccr2⁻/⁻* lasered (**C**) mice. Pericytes (**D**) and endothelial cells (**E**) were unaffected by laser treatment nor *Ccr2*-deficiency ($N = 3$–4 per group).

Comparisons between unlasered wildtype, lasered wildtype, and lasered *Ccr2⁻/⁻* mice were made by 1-way ANOVA followed by Tukey's multiple comparisons test because there were three groups. Comparisons between PBS and propranolol were made using the Mann-Whitney test because the data were non-parametrically distributed.

RESULTS

The choroidal sprouting ex vivo model is a 3-dimensional tissue model of angiogenesis that includes endothelial cells, pericytes, retinal pigment epithelium (RPE), and tissue resident choroidal macrophages.[17] We previously showed that propranolol reduces VEGF and IL-6 expression in primary mouse choroidal endothelial cells, pericytes, RPE, and microglia cell lines, all of which express beta-ARs.[9,10] To further test the anti-angiogenic properties of propranolol, we performed a dose-response analysis of propranolol in the choroidal sprouting assay. Angiogenic sprouts were first visible on Day 3, and representative images of vehicle- and propranolol-treated choroidal explants are shown in Figures 1A through 1F. We identified a dose-dependent reduction in choroidal angiogenesis from 14% to 41% with 50 nM to 5 μM propranolol (Fig. 1G, $P < 0.001$ for 5 μM). Propranolol was nearly as effective as the 56% inhibition obtained with the multi-receptor tyrosine kinase inhibitor sunitinib, which potently inhibits VEGF receptor 2 signaling (Fig. 1G; $P < 0.0001$).

Our prior report demonstrated that propranolol inhibits laser-induced CNV by 50% in female mice using immunofluorescence (IF) staining.[9] However, we did not investigate male mice or the effect size using fluorescein angiography (FA). Here, we performed laser-induced CNV in male and female mice undergoing daily intraperitoneal injection of vehicle (PBS) or propranolol (20 mg/kg) starting on the day of laser treatment. Propranolol reduced laser-induced CNV area by 50% by both FA and IF (Fig. 2H–2I; $P = 0.01$ for both). Propranolol

had no effect upon FA leakage (Fig. 2G) or rate of CNV formation (Fig. 2J) in female mice. In contrast, propranolol had no effect upon CNV area by FA or IF (Fig. 2L–2M) in male mice. Interestingly, propranolol caused more Grade 3–4 lesions on FA in male mice (Fig. 2K; $P < 0.01$) without changing Grade 1 lesions or CNV rate (Fig. 2N). These data suggest that propranolol reduced the area of lesions without affecting their FA leakage characteristics in female mice. Alternatively, propranolol caused more lesions with leakage in male mice, but the size of the lesions was not significantly different. These data suggest a sex-specific response to beta-AR driven CNV inhibition, although the mechanism is unknown.

We recently identified that intravitreal beta2-AR inhibition reduces CNV area and ocular IL-6 levels without affecting the expression of VEGF.[10] Macrophages, which are known to produce high levels of IL-6 and express beta-ARs,[13] were examined in the choroidal sprouting ex vivo model with an adaptation using bone marrow-derived macrophages (BMDMs). The addition of 10,000 and 20,000 BMDMs increased choroidal angiogenesis by 127% ($P < 0.01$) and 146% ($P < 0.0001$) on Day 7, respectively (Fig. 3J). To test the effect of propranolol on BMDM-stimulated choroidal angiogenesis, we added propranolol in conjunction with monocyte addition. We found that propranolol alone mildly reduced choroidal angiogenesis by 10% without BMDMs ($P = $ NS; Fig. 3K). Alternatively, BMDMs stimulated angiogenesis by 118% ($P < 0.001$), and this effect was attenuated in the presence of propranolol ($P = $ NS versus control, $P < 0.05$ versus BMDM; Fig. 3K). These data suggest that monocytes or monocyte-derived macrophages may regulate the effects of propranolol on choroidal angiogenesis.

C-C motif chemokine receptor 2 (CCR2) is a receptor that is necessary for emigration of classical monocytes from the bone marrow into the circulation and for recruitment of monocytes to sites of tissue injury.[18] We subjected *Ccr2⁻/⁻* mice to laser-induced CNV and tested whether propranolol was capable of
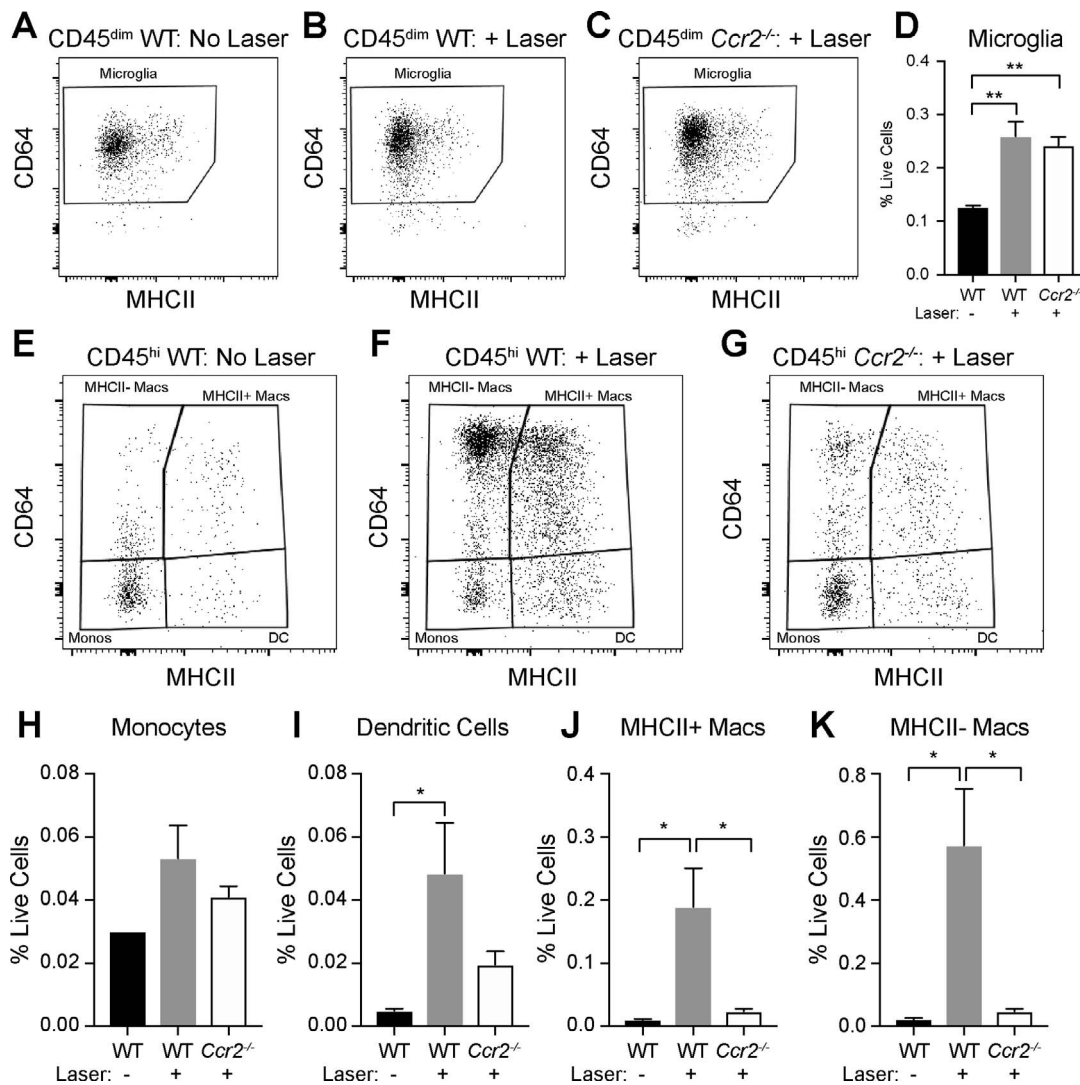
FIGURE 7. MHCII$^+$ Macs and MHCII$^-$ Macs are the primary CCR2-dependent tissue infiltrating cells. Representative flow cytometry plots of CD45^{dim} cells in WT unlasered (**A**), WT lasered (**B**), and *Ccr2*$^{-/-}$ lasered (**C**) mice. (**D**) Microglia increased with laser treatment in WT and *Ccr2*$^{-/-}$ mice compared to WT unlasered mice. Representative flow cytometry plots of CD45^{high} cells in WT unlasered (**E**), WT lasered (**F**), and *Ccr2*$^{-/-}$ lasered (**G**) mice. (**H**) Ocular circulating monocytes were non-significantly increased by laser treatment in wildtype (WT) mice, but unchanged in *Ccr2*$^{-/-}$ mice. (**I**) Dendritic cells (DC) increased with laser in WT mice and were non-significantly reduced by *Ccr2*-deficiency. MHCII$^+$ (**J**) and MHCII$^-$ (**K**) Macs dramatically increased with laser in WT mice and this effect was completely blocked in *Ccr2*$^{-/-}$ mice ($N = 3$–4 per group *$P < 0.05$, **$P < 0.01$).

inhibiting CNV in female mice. Propranolol treatment had no effect on CNV area or CNV rate in female *Ccr2*$^{-/-}$ mice (Figs. 4A–C). These data demonstrate that monocyte-derived macrophages are necessary for propranolol-driven CNV inhibition.

Since macrophages are known to be heterogenous, we examined the different populations of tissue macrophages via flow cytometric analysis on Day 3, the peak of macrophage recruitment.[12] Microglia were identified in the CD45^{dim} group as CD64$^+$ and predominantly MHCII^{low} (Fig. 5). In the CD45^{high} group, we identified CD64$^-$MHCII$^-$ monocytes, CD64$^-$MHCII$^+$ dendritic cells (DC), and two populations of macrophages (Fig. 5): CD64$^+$MHCII$^-$ macrophages (MHCII$^-$ Macs) and CD64$^+$MHCII$^+$ macrophages (MHCII$^+$ Macs).

To determine which cellular populations were CCR2-dependent during laser-induced CNV, we compared female untreated and lasered wildtype (WT) mice with female lasered *Ccr2*$^{-/-}$ mice using multi-parameter flow cytometry on Day 3. There was no change in the percent or numbers of pericytes, endothelial cells, or monocytes regardless of treatment or genotype (Figs. 6D, 6E, 7H). DC numbers increased with laser treatment by 9.9-fold ($P < 0.05$) in WT mice and were non-significantly increased 4-fold in *Ccr2*$^{-/-}$ lasered mice (Fig. 7I). We detected 2.1- and 1.9-fold more microglia in lasered WT ($P < 0.01$) and *Ccr2*$^{-/-}$ ($P < 0.01$) mice, respectively (Fig. 7D). MHCII$^-$ and MHCII$^+$ macrophages increased 26.2- ($P < 0.05$) and 18.3-fold ($P < 0.05$) after laser treatment, respectively, and this effect was completely ablated in lasered *Ccr2*$^{-/-}$ mice (Figs. 7J–7K). These data suggest that MHCII$^-$ and MHCII$^+$ macrophages are the predominant CCR2-dependent tissue infiltrating cells during laser-induced CNV.

Next, we compared female, lasered WT mice treated with vehicle or propranolol on Day 3 to determine if propranolol affects macrophage recruitment to laser lesions. We found no change in pericytes or endothelial cells between PBS- and propranolol-treated mice (Figs. 8A, 8B). Monocytes, DC, and microglia numbers were non-significantly increased by 1.5-fold ($P = 0.62$), 2.1-fold ($P = 0.12$), and 1.2-fold ($P = 0.10$), respectively, with propranolol treatment (Figs. 8C–E). Howev-
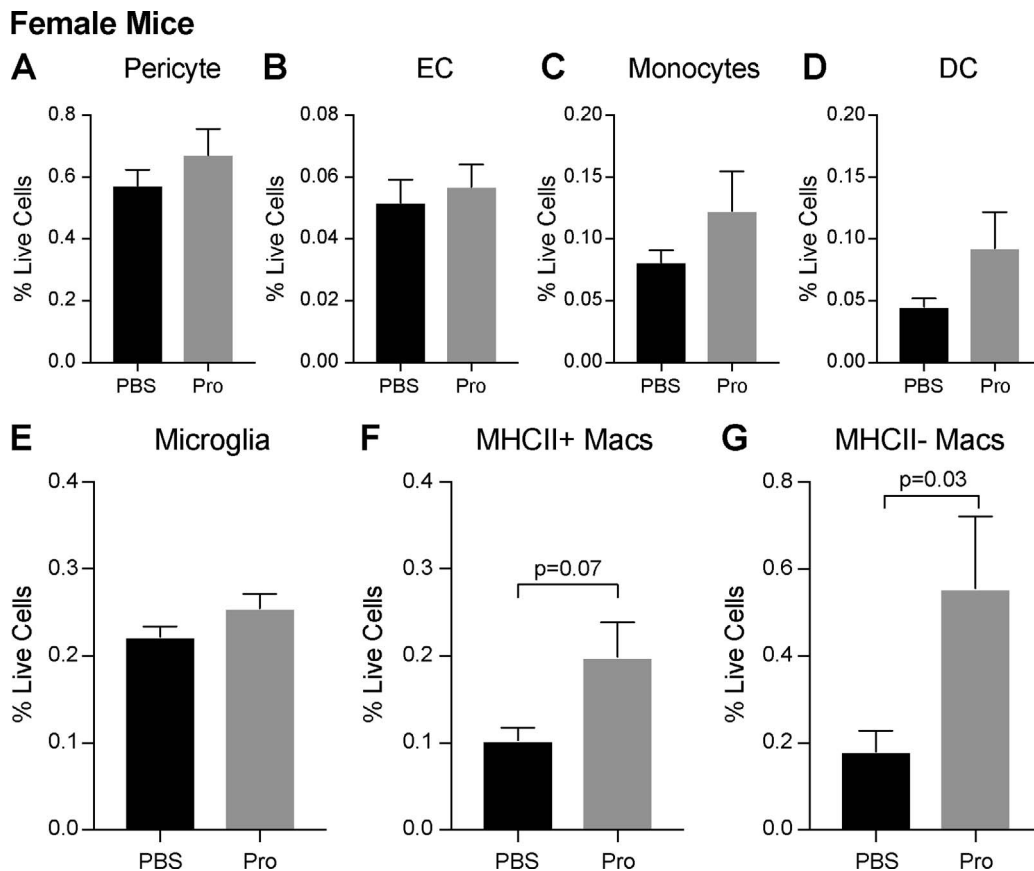
Female Mice

FIGURE 8. Propranolol increased MHCII⁻ Macs during laser-induced CNV in female mice. Propranolol had no effect upon pericytes (**A**), endothelium (**B**), monocytes (**C**), dendritic cells (**D**), or microglia (**E**). (**F, G**) Propranolol treatment increased MHCII⁺ Macs ($P = 0.07$) and MHCII⁻ Macs ($P = 0.03$) on Day 3 ($N = 9$–10 per group).

er, we detected 3.1-fold more MHCII⁻ macrophages ($P < 0.05$) and 1.9-fold more MHCII⁺ macrophages ($P = 0.07$) with propranolol treatment (Figs. 8F, 8G).

Finally, we compared male, lasered WT mice treated with vehicle or propranolol on Day 3 to determine if recruitment of MHCII⁻ and MHCII⁺ macrophages is responsible for the lack of CNV inhibition in male propranolol-treated mice. Similar to female mice, there was no significant differences in the numbers of pericytes, endothelial cells, microglia, DC, or monocytes between male vehicle and propranolol-treated mice (Figs. 9A–9E). In contrast to female mice, male propranolol-treated mice demonstrated no change in the numbers of MHCII⁻ nor MHCII⁺ macrophages (Figs. 9F, 9G). These data suggest that beta-AR antagonist-driven recruitment of MHCII⁻ and MHCII⁺ macrophages explains the sex-specific differences between male and female mice.

DISCUSSION

Beta-AR inhibitors are clinically used for many ophthalmic indications including severe hemangioma of infancy,[1] retinopathy of prematurity,[2,3] and persistent intraretinal or subretinal fluid in patients with neovascular AMD[6] or retinal vein occlusion.[19] In this report, we used two models of choroidal angiogenesis to study these effects further: the ex vivo choroidal sprouting assay and the laser-induced CNV model. We found that propranolol inhibits angiogenesis in both of these models (Figs. 1, 2). In the laser-induced CNV model, we treated the mice with propranolol directly before laser injury. Because laser-induced CNV does not develop for several days,

this is both a prevention and treatment study. Since there is no change in CNV formation or Grade 1 FA leakage, the data do not suggest that propranolol prevented CNV formation. In epidemiologic studies beta-AR blockers have been shown to both increase[20] and decrease[21] the incidence of nAMD diagnoses. Therefore, our data do not clarify this controversial subject. Instead, our data demonstrate that propranolol decreased CNV size without affecting leakage characteristics in female mice, suggesting a treatment effect. These data are supported by multiple clinical studies that showed improved retinal thickness with dorzolamide-timolol in conjunction with anti-VEGF treatment in nAMD patients.[5,6]

Despite their experimental and clinical efficacy, the mechanism by which beta-AR blockers inhibit angiogenesis is poorly understood. We previously demonstrated that intravitreal beta2-AR inhibition reduces laser-induced CNV and is correlated with decreased ocular IL-6 levels with no change in VEGF levels.[10] Because IL-6 is produced by macrophages and monocyte-derived macrophages are necessary for laser-induced CNV,[11] we sought to determine if monocyte-derived macrophages are critical for the anti-angiogenic effects of beta-AR inhibition. Additionally, we showed that addition of BMDMs increased choroidal angiogenesis (Fig. 3J), and this effect was ablated by propranolol treatment (Fig. 3K). In confirmation of the critical role of monocyte-derived macrophages, we demonstrated that propranolol no longer decreased laser-induced CNV in $Ccr2^{-/-}$ mice, presumably due to the lack of monocyte-derived macrophages (Fig. 4). These data illustrate that CCR2-dependent monocyte-derived macrophages are necessary for beta-AR driven CNV inhibition.
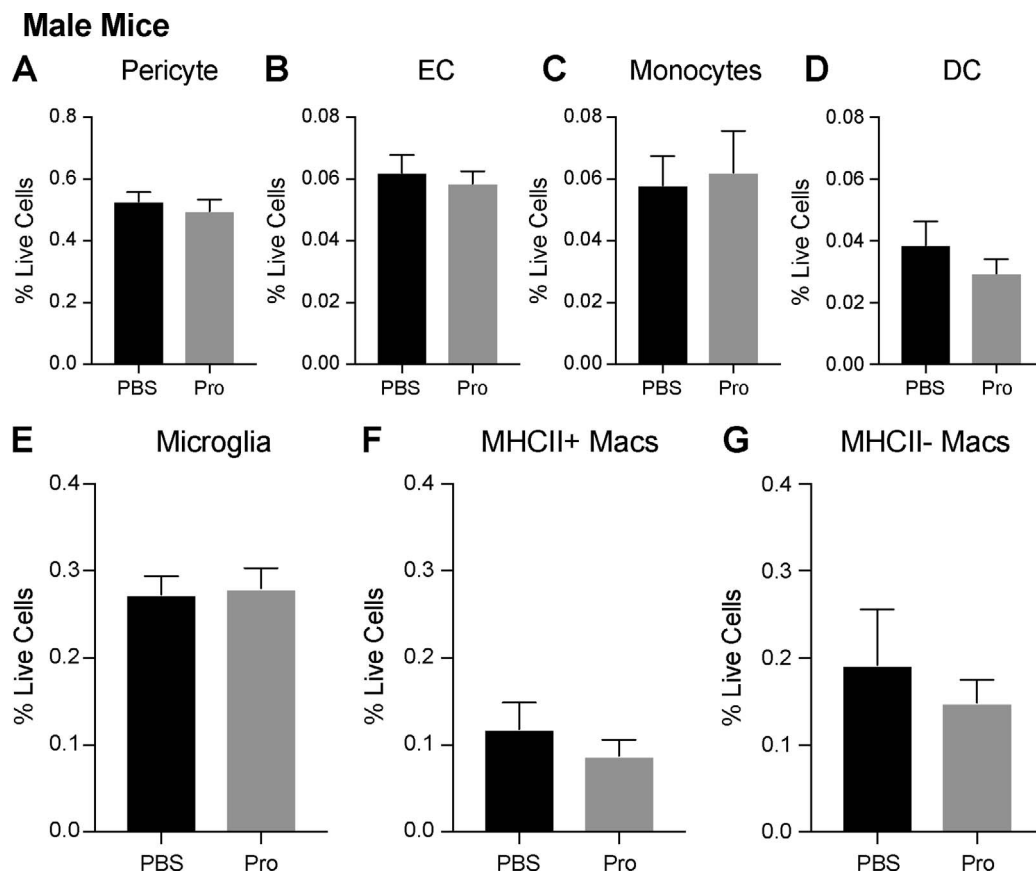
Male Mice

FIGURE 9. Propranolol has no effect upon ocular mononuclear phagocytes during laser-induced CNV in male mice. Propranolol had no effect upon pericytes (**A**), endothelium (**B**), monocytes (**C**), dendritic cells (**D**), microglia (**E**), MHCII+ Macs (**F**), or MHCII− Macs (**G**, $N = 7$ per group).

Because loss of monocyte-derived macrophages reduces the laser-induced CNV area,[11] we tested whether propranolol inhibits recruitment of monocyte-derived macrophages to the laser injury. This mechanism of action is supported by a cardiac injury model where the beta2-AR is necessary for CCR2 expression and leukocyte infiltration to the injury site.[22] We measured mononuclear phagocytes on Day 3 after laser injury, the peak of macrophage recruitment.[12] After laser treatment, MHCII− and MHCII+ Macs are the primary CCR2-dependent monocyte-derived macrophage types recruited to the injury site (Fig. 7). Propranolol did not change the endothelial cell, pericyte, or monocyte numbers on Day 3, which was expected because the CNV has not formed on Day 3, and the monocytes detected are not tissue recruited but in the ocular circulation. Importantly, beta-AR blockade increased, rather than decreased, the number of MHCII− and MHCII+ Macs after laser injury compared to vehicle control in female mice (Fig. 8). These data clearly display that reduction of monocyte-derived macrophage recruitment is not the mechanism by which beta-AR blockade inhibits CNV.

Although *Ccr2*-deficiency causes reduced macrophage infiltration to laser lesions (Fig. 7) and decreased CNV area,[11] both pro-angiogenic and anti-angiogenic macrophages have been described. For example, Kelly et al.[23] reported that aged macrophages display a pro-angiogenic phenotype that is regulated by increased interleukin-10 expression. Alternatively, intravitreal injection of isolated splenic macrophages from young mice[23] or M1-polarized macrophages[24] are capable of inhibiting laser-induced CNV area. Furthermore, IL-10 knockout mice demonstrate decreased CNV area and increased macrophage numbers,[25] demonstrating three examples of anti-angiogenic ocular macrophages. Therefore, beta-AR blockade may cause either more anti-angiogenic macrophages to be recruited to the laser lesion or a shift in macrophage gene expression and phenotype toward an anti-angiogenic subtype. In support of this anti-angiogenic mechanism, beta-AR agonism increases *Vegfa* expression in bone marrow-derived macrophages.[26] Future studies will investigate if beta-AR blockade decreases the expression of pro-angiogenic genes, such as *Vegfa*, in monocyte-derived macrophages.

It was surprising that male mice did not demonstrate reduced CNV area (Fig. 2) nor increased macrophage recruitment to laser injury (Fig. 9) during beta-AR blockade. Epidemiologic studies are variable, but several reports show a positive association between female sex and AMD risk.[27] Furthermore, the incidence of late stage AMD, including neovascularization and geographic atrophy, was 38% higher in women in a meta-analysis.[28] Although women have a longer life expectancy and are thus more likely to get age-related diseases, both studies remark upon the sex predilection being larger than expected for age differences. Additionally, there are sex-specific differences in macrophage function, including activation, phagocytic capacity, and IL-10 production.[29] Interestingly, IL-10 is a pro-angiogenic cytokine.[25] Beta-AR blockade may influence a sex-specific inflammatory component of the multifactorial disease pathogenesis of AMD, possibly including IL-10 production.

In conclusion, propranolol inhibits choroidal angiogenesis in both the ex vivo choroidal sprouting assay and the in vivo laser-induced CNV model (Figs. 1, 2). Furthermore, monocyte-derived macrophages are critical for beta-AR blockade inhibition of laser-induced CNV (Figs. 3, 4). Finally, we displayed that

propranolol increased macrophage tissue infiltration after laser injury only in female mice (Figs. 8, 9). Our data suggest a mechanism where beta-AR antagonism increases monocyte-derived macrophage recruitment to the laser lesion, which is necessary for reduction in laser-induced CNV, implicating the anti-angiogenic nature of beta-AR blocker-recruited monocyte-derived macrophages.

Acknowledgments

References

1. Léauté-Labrèze C, Dumas de la Roque E, Hubiche T, Boralevi F, Thambo J-B, Taïeb A. Propranolol for severe hemangiomas of infancy. *N Engl J Med*. 2008;358:2649–2651.

2. Filippi L, Cavallaro G, Bagnoli P, et al. Oral propranolol for retinopathy of prematurity: risks, safety concerns, and perspectives. *J Pediatr*. 2013;163:1570–1577.

3. Filippi L, Cavallaro G, Berti E, et al. Propranolol 0.2% eye micro-drops for retinopathy of prematurity: a prospective Phase IIB study. *Front Pediatr*. 2019;7:180.

4. Rahimy E, Ying G-S, Pan W, Hsu J. Effect of intraocular pressure-lowering medications on neovascular age-related macular degeneration treatment outcomes in the comparison of age-related macular degeneration treatment trials. *Retina*. 2018;39:636–647.

5. Lee JH, Lee SC, Byeon SH, Koh HJ, Kim SS, Lee CS. Efficacy of adjuvant topical dorzolamide-timolol in patients with neovascular age-related macular degeneration refractory to anti-vascular endothelial growth factor therapy. *Retina*. 2019;39:1953–1958.

6. Sridhar J, Hsu J, Shahlaee A, et al. Topical dorzolamide-timolol with intravitreous anti–vascular endothelial growth factor for neovascular age-related macular degeneration. *JAMA Ophthal*. 2016;134:437.

7. Chim H, Armijo BS, Miller E, Gliniak C, Serret MA, Gosain AK. Propranolol induces regression of hemangioma cells through HIF-1α–mediated inhibition of VEGF-A. *Ann Surg*. 2012;256:146–156.

8. Przewratil P, Kobos J, Wnęk A, et al. Serum and tissue profile of VEGF and its receptors VGFR1/R2 in children with infantile hemangiomas on systemic propranolol treatment. *Immunol Lett*. 2016;175:44–49.

9. Lavine JA, Sang Y, Wang S, Ip MS, Sheibani N. Attenuation of choroidal neovascularization by β(2)-adrenoreceptor antagonism. *JAMA Ophthalmol*. 2013;131:376–382.

10. Lavine JA, Farnoodian M, Wang S, et al. β2-Adrenergic receptor antagonism attenuates CNV through inhibition of VEGF and IL-6 expression. *Invest Ophthalmol Vis Sci*. 2017;58:299–308.

11. Tsutsumi C. The critical role of ocular-infiltrating macrophages in the development of choroidal neovascularization. *J Leukoc Biol*. 2003;74:25–32.

12. Sakurai E, Anand A, Ambati BK, van Rooijen N, Ambati J. Macrophage depletion inhibits experimental choroidal neovascularization. *Invest Ophthalmol Vis Sci*. 2003;44:3578–3585.

13. Chiarella SE, Soberanes S, Urich D, et al. β2-Adrenergic agonists augment air pollution–induced IL-6 release and thrombosis. *J Clin Invest*. 2014;124:2935–2946.

14. Krzystolik MG, Afshari MA, Adamis AP, et al. Prevention of experimental choroidal neovascularization with intravitreal anti-vascular endothelial growth factor antibody fragment. *Arch Ophthalmol*. 2002;120:338–346.

15. Zambarakji HJ, Nakazawa T, Connolly E, et al. Dose-dependent effect of pitavastatin on VEGF and angiogenesis in a mouse model of choroidal neovascularization. *Invest Ophthalmol Vis Sci*. 2006;47:2623–2629.

16. O'Koren EG, Mathew R, Saban DR. Fate mapping reveals that microglia and recruited monocyte-derived macrophages are definitively distinguishable by phenotype in the retina. *Sci Rep*. 2016;9:1–12.

17. Shao Z, Friedlander M, Hurst CG, et al. Choroid sprouting assay: an ex vivo model of microvascular angiogenesis. *PLoS One*. 2013;8:e69552–11.

18. Kratofil RM, Kubes P, Deniset JF. Monocyte conversion during inflammation and injury. *Arterioscler Thromb Vasc Biol*. 2017;37:35–42.

19. Obeid A, Hsu J, Ehmann D, et al. Topical dorzolamide-timolol with intravitreous anti-vascular endothelial growth factor for retinal vein occlusion: a pilot study [published online ahead of pring June 1, 2018]. *Retin Cases Brief Rep*. doi:10.1097/ICB.0000000000000752.

20. Yeung L, Huang T-S, Lin Y-H, Hsu K-H, Chien-Chieh Huang J, Sun C-C. β-blockers and neovascular age-related macular degeneration. *Ophthalmology*. 2017;124:409–411.

21. Kolomeyer AM, Maguire MG, Pan W, VanderBeek BL. Systemic beta-blockers and risk of progression to neovascular age-related macular degeneration. *Retina*. 2019;39:918–925.

22. Grisanti LA, Traynham CJ, Repas AA, Gao E, Koch WJ, Tilley DG. β2-adrenergic receptor-dependent chemokine receptor 2 expression regulates leukocyte recruitment to the heart following acute injury. *Proc Natl Acad Sci U S A*. 2016;113:15126–15131.

23. Kelly J, Khan AA, Yin J, Ferguson TA, Apte RS. Senescence regulates macrophage activation and angiogenic fate at sites of tissue injury in mice. *J Clin Invest*. 2007;117:3421–3426.

24. Zandi S, Nakao S, Chun K-H, et al. ROCK-isoform-specific polarization of macrophages associated with age-related macular degeneration. *Cell Rep*. 2015;10:1173–1186.

25. Apte RS, Richter J, Herndon J, Ferguson TA. Macrophages inhibit neovascularization in a murine model of age-related macular degeneration. *PLoS Med*. 2006;3:e310.

26. Lamkin DM, Ho H-Y, Ong TH, et al. β-Adrenergic-stimulated macrophages: comprehensive localization in the M1-M2 spectrum. *Brain Behav Immun*. 2016;57:338–346.

27. Pennington KL, DeAngelis MM. Epidemiology of age-related macular degeneration (AMD): associations with cardiovascular disease phenotypes and lipid factors. *Eye Vis (Lond)*. 2016: 22;3:34.1–20.

28. Rudnicka AR, Kapetanakis VV, Jarrar Z, et al. Incidence of late-stage age-related macular degeneration in American whites: systematic review and meta-analysis. *Am J Ophthalmol*. 2015;160:85–93.

29. Klein SL, Flanagan KL. Sex differences in immune responses. *Nat Rev Immunol*. 2016;16:626–638.